SAND2018-12553C

Threshold for the torus instability of arched, line-tied flux ropes

Andrew Alt[1], Clayton E. Myers[2], Hantao Ji[1]

[1] Princeton University, [2] Sandia National Laboratories

60th Annual Meeting of the APS Division of Plasma Physics

Abstract

Coronal mass ejections occur when long-lived magnetic flux ropes anchored to the solar surface destabilize and erupt away from the Sun. One mechanism that drives this eruption is the ideal magnetohydrodynamic torus instability [1]. The torus instability has previously been considered in axisymmetric fusion devices where instability criterion is given by the decay index of the confining magnetic field, $n = -\frac{R}{B}\frac{\partial B}{\partial R} > n_{cr}$, where $n_{cr} \approx 1.5$ in the large aspect ratio limit. In recent laboratory experiments performed on the Magnetic Reconnection Experiment (MRX), however, the critical decay index in solar-relevant, line-tied flux ropes was instead found to be $n_{cr} \approx 0.8$ [2]. In this work, we investigate how line-tying and aspect ratio effects modify the predicted torus instability criterion. We then compare these predictions to the MRX flux rope eruption database. This work motivates future laboratory experiments in continued investigation of line-tied flux rope eruption mechanisms, including the role of magnetic self-organization in erupting and non-erupting flux ropes.

Background

- Protrusions of magnetic field and plasma from the Solar surface often result in the formation of long, thin flux ropes (FR).
- These ropes are long-lived but can violently erupt, causing solar flares or coronal mass ejections (CME).
- Understanding the stability of these FR is necessary to predict CMEs.
- Foot points of the FRs are anchored to the conductive Solar surface through line-tying, affecting their stability properties.
- In order for an eruption to occur, the FR must be unstable enough to push through the external magnetic fields.
- One instability that can trigger CMEs is the torus instability.

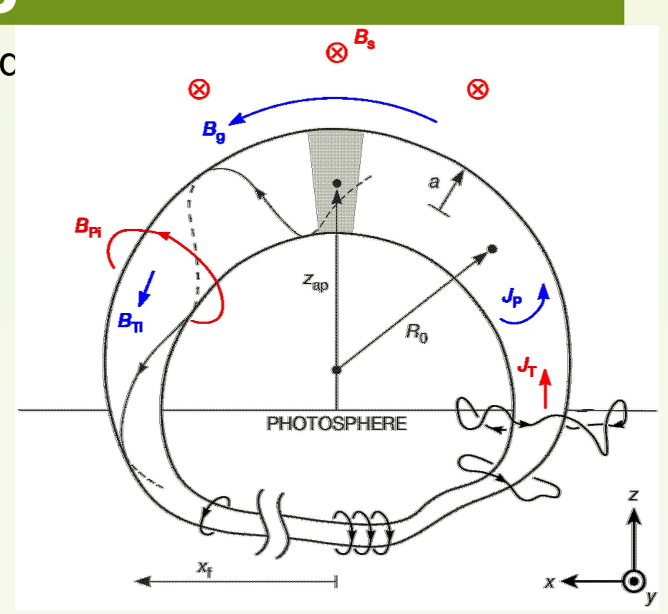

A cartoon depicting the fields and currents associated with a flux rope. Figure reproduced from Ref. [3].

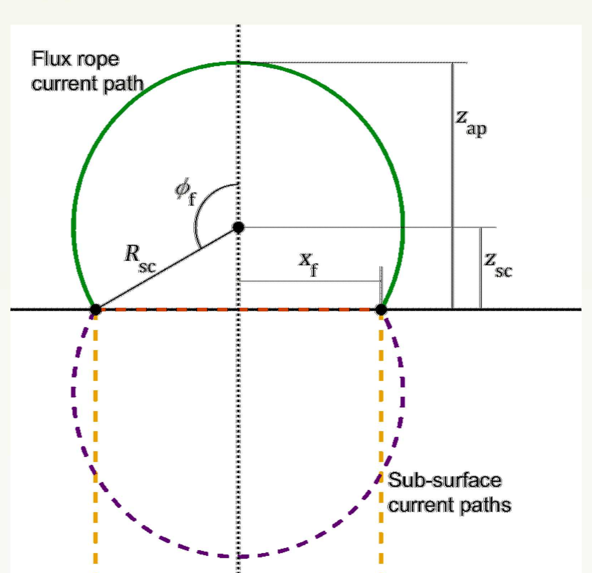

A diagram of the line-tied, shifted-circle model we use to estimate the shape of a flux rope. Different sub-surface closures are shown. Image currents for the Solar case and different orientations of fixed wires for the lab case.

Simple FR model

- The FRs are modeled as a partial circle with fixed foot points at $x = \pm x_f$.
- The FR is characterized by one scalar, the apex height z_{ap}.
- The radius of curvature is then $R_{sc} = \frac{z_{ap}^2 + x_f^2}{2 z_{ap}}$.
- The return path depends on the system. Image currents for the Solar case and fixed wires in the lab.

Experiment

- Flux ropes were created in the MRX vessel by creating a discharge between two electrodes. The foot points are line-tied to these conductive electrodes.
- The vacuum fields were controlled by 4 independent coils.
- Plasma current is injected quasi-statically by a capacitor bank.
- A 2D magnetic probe array is used to measure the fields in the rope during a discharge. The array can be rotated to measure in different planes of the FR.

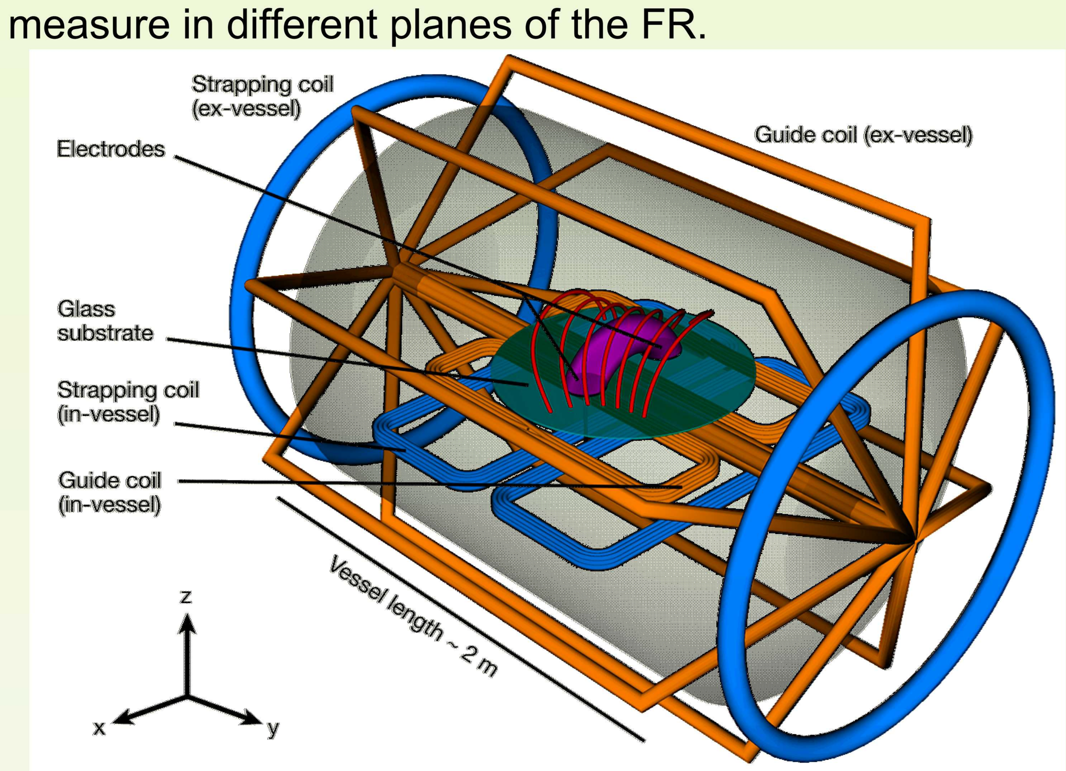

A schematic of the MRX vessel configuration during the flux rope experiments. Figure reproduced from Ref. [2].

Experimental Parameters	
Magnetic field (B)	$300 - 500$ G
Neutral density (n_n)	$\sim 5 \times 10^{14}\,\mathrm{cm}^{-3}$
Electron density (n_e)	$0.5 - 1 \times 10^{14}\,\mathrm{cm}^{-3}$
Electron temperature (T_e)	$3 - 5$ eV
FR scale length (L)	0.5 m
Alfvén speed (v_A)	$65 - 150$ km/s
Alfvén time (τ_A)	$3 - 8\ \mu s$
Driving time (τ_D)	$\sim 150\ \mu s$
Resistive time (τ_R)	$0.8 - 2$ ms

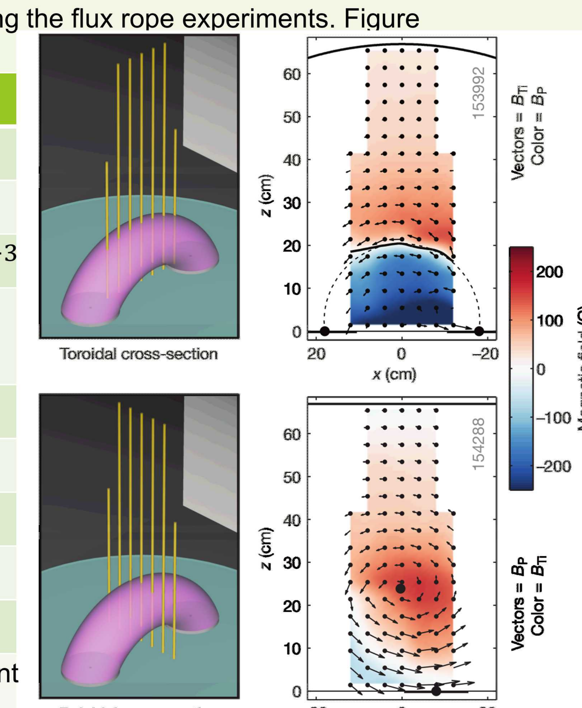

Example data from 2 shots with the probe array in different orientations. Figure reproduced from Ref. [2].

Axisymmetric Hoop Force

- The magnetic energy is $W = \frac{1}{2} I^2 L$
- The inductance of a large aspect ratio torus $L \approx \mu_0 R \left[\ln\left(\frac{8R}{a}\right) - 2 + \frac{\ell_i}{2}\right] \equiv \mu_0 R \ell$
- The internal inductance is $\ell_i = \langle B_p^2 \rangle / B_{pa}^2$. $\ell_i = \frac{1}{2}$ for a uniform current distribution.
- The hoop force per unit length is then $F_h = \frac{-1}{2\pi R}\frac{\partial W}{\partial R} = \frac{I^2}{4\pi R}\frac{\partial L}{\partial R} = \frac{\mu_0 I^2}{4\pi R}(\ell + 1)$
- The poloidal flux $\Phi = LI$ has been held constant.

Force	Source	Expression
Hoop (F_h)	$+J_T B_{pi}$	$\frac{\mu_0 I_T^2}{4\pi R}\left[\ln\left(\frac{8R}{a}\right) - 1 + \frac{\ell_i}{2}\right]$
Correction (F_{cr})		$C\frac{\mu_0 I_T^2}{4\pi R}$
Strapping (F_s)	$-J_T B_{pi}$	$-I_T B_s$
Tension (F_t)	$-J_p(B_g + B_{Ti})$	$-\frac{1}{2}\frac{\mu_0 I_T^2}{4\pi R}\left[\frac{\langle B_T^2 \rangle - B_g^2}{B_{pa}^2}\right] \approx -\frac{1}{2}\frac{\mu_0 I_T^2}{}$

Torus Instability

Consider a FR in equilibrium

$$F_h + F_s + F_t + F_{cr}\Big|_{z=z_{ap}} = 0$$

The torus instability occurs when

$$\frac{\partial F}{\partial z} = \frac{\partial}{\partial z}(F_h + F_s + F_t + F_{cr})\Big|_{z=z_{ap}} > 0$$

These derivatives are

$$\frac{\partial F_h}{\partial z} = -\frac{F_h}{z}\left[2n_I - n_R + \frac{1}{\ell+1}n_A + \frac{\ell_i}{2(\ell+1)}n_{\ell_i}\right]$$

$$\frac{\partial F_s}{\partial z} = -\frac{F_s}{z}[n_I + n_s]$$

$$\frac{\partial F_t}{\partial z} = -\frac{F_t}{z}[2n_I - n_R]$$

$$\frac{\partial F_{cr}}{\partial z} = -\frac{F_{cr}}{z}[2n_I - n_R + n_C]$$

Where $n_s = -\frac{z}{B_s}\frac{\partial B_s}{\partial z}$ is the decay index of the strapping field and other decay indices are similarly defined. In the shifted circle model, $n_R = \frac{x_f^2 - z^2}{x_f^2 + z^2}$.

With the equilibrium condition, the FR is unstable iff

$$n_s > -n_R + n_I + \frac{2n_A}{2\ell + 1 + 2C} + \frac{2\ell_i n_{\ell_i}}{2\ell + 1 + 2C} + \frac{2Cn_C}{2\ell + 1 + 2C}$$

In the solar case, conservation of poloidal flux constrains the decay index of the current to $n_I \approx 0.5$. However, due to the large inductance of the capacitor bank, in the lab the current was not able to change and $n_I = 0$.

For a full, large-aspect-ratio torus, $n_R = -1$, and $\ell \gg 1$, so $n_{cr} \approx 1.5$.

By analytically or numerically analyzing n_C, the critical decay index for a line-tied FR can be determined.

Numerical Hoop Force

In order to better quantify the effect of the shifted circle model on the torus instability, the hoop force can be numerically evaluated and from that, a critical decay index determined.

The hoop force is calculated using Biot-Savart law and different sub-surface closures:

1. A horizontal wire connecting the foot points
2. Vertical wires going to infinity from each foot point
3. An image current.

The critical decay index can then be calculated as

$$n_{cr} = n_I - \frac{z\,F_N}{F_h + F_t}\frac{\partial}{\partial z}\left(\frac{F_h + F_t}{F_N}\right)$$

Here the forces are normalized to $F_N = \frac{\mu_0 I^2}{4\pi x_f}$. n_{cr} depends largely on the FR height and the assumed aspect ratio.

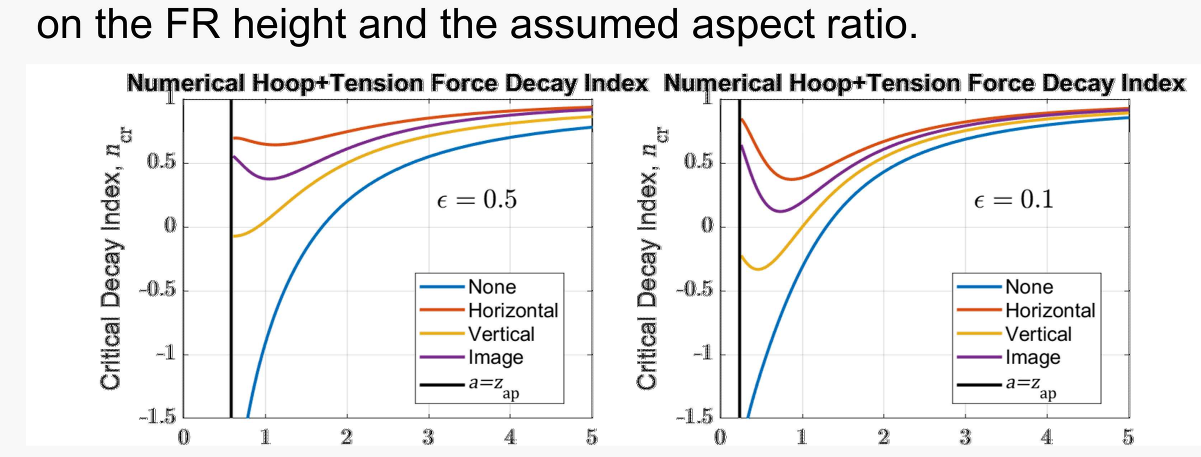

Numerically calculated hoop force decay index based on a shifted circle model. For these the inverse aspect ratio of the FR was held constant $\epsilon = a/R_0 = 0.5, 0.1$. The black line denotes the minimum z for which this makes sense. Below that point, the FR and the wires or image current

Sandia National Laboratories is a multimission laboratory managed and operated by National Technology & Engineering Solutions of Sandia, LLC, a wholly owned subsidiary of Honeywell International Inc., for the U.S. Department of Energy's National Nuclear Security Administration under contract DE-NA0003525.

Force Decay Index

- By experimentally evaluating the force as a function of apex position, the stability of different shots can be verified.
- The slope of $F(z)$ during the rise of the FR show its stability.
- In each case, the force becomes nonlinear once the FR has risen too far.
- In the stable case, an enhanced tension force stops the total force from decaying as the rope falls.

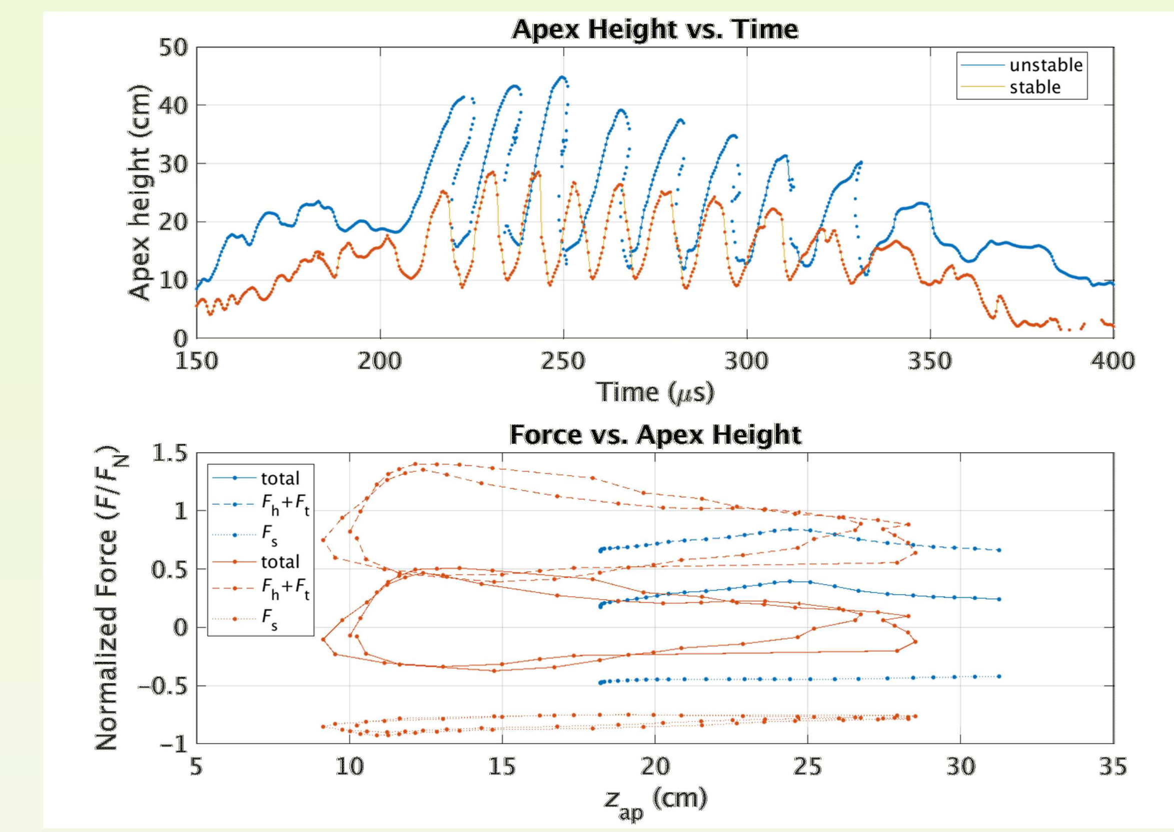

The experimentally measured forces for a shot that was torus unstable and one that was torus stable but kink unstable. The slope of $F(z)$ is consistent with the analytical prediction.

Conclusions

The stability properties of Solar flux ropes are important for understanding the cause and evolution of coronal mass ejections. The torus instability is one MHD instability that can drive FRs to eruption. While the decay index of the strapping magnetic field has been shown to not be a sufficient condition for eruption [2] it has been shown to strongly correlate with CME activity in Solar observations [4]. The previously observed critical index of $n_{cr} \approx 0.8$ has been verified numerically with a simplified FR model. Experimental measurements of the forces on a FR during a perturbation verify the theory of the torus instability. The enhancement of the tension force while the FR was falling was unexpected and hints at flaws in our assumptions in deriving this force.

Future work is planned with experimental upgrades that will allow a larger parameter space to be investigated. These upgrades will also allow us to quasi-statically vary the vacuum fields to observe destabilization of a flux rope. This will be a closer analog to Solar FR eruptions and will allow us to better probe the instability conditions of a line-tied flux rope.

References

[1] B. Kliem and T. Török, Phys. Rev. Lett. **96**, 255002 (2006)
[2] Myers et al., Nature **528**, 526 (2015)
[3] Myers et al., Phys. Plasmas **23** 112102 (2016)
[4] J. Jing, et al., Astrophys. J. **864**, 138 (2018)

*This work is funded by DoE contract numbers DE-AC02-09CH11466 (Princeton) and DE-NA0003525 (Sandia).

Contact Information
aalt@pppl.gov